The KT phase transition and the XY model

physics760 - Computational physics

Lennart Voorgang

March 26, 2025

Contents

1 Introduction **1**

2 Numerical Methods **1**
2.1 Monte Carlo Metropolis-Hastings Algorithm 1
2.2 Bootstrap Analysis 2
2.3 Implementation 2

3 Results **2**
3.1 Energy per Spin 2
3.2 Magnetization per Spin 2
3.3 Specific Heat per Spin 3
3.4 Magnetic Susceptibility per Spin 3
3.5 Critical Temperature T_C 6
3.6 Vortices 7
3.7 Performance 7
3.7.1 Schedueling 7
3.7.2 Test 7
3.7.3 Critical slowing down 7

4 Conclusion **7**

List of Figures **I**

References **II**

1 Introduction

The perhaps most well known model for the magnetization of lattice structures is the Ising spin model. It describes the total magnetization of a lattice as the superposition of all spins $\sigma_i = \pm 1$ on the lattice.

XY model One can now go and generalize the problem from a $\mathbb{Z}_2$ symmetry to a continous $U(2)$ symmetry. This model is called the XY model and describes the spins as two dimensional vectors on the unit circle

$$\sigma_i = \begin{pmatrix} \cos\theta_i \\ \sin\theta_i \end{pmatrix} \tag{1}$$

parametrized by the angle $\theta_i \in [0, 2\pi)$. The Hamiltonian for this system is thus given as

$$H = -J \sum_{\langle i,j \rangle} s_i \cdot s_j = -J \sum_{\langle i,j \rangle} \cos(\Delta\theta) \tag{2}$$

where $\Delta\theta = \theta_i - \theta_j$ is the angle between two spins and J the interaction strength. The $\langle i, j \rangle$ notation is used to indicate a nearest neighbour approximation. The partition sum for such a system is given by

$$Z = \sum \exp(-\beta H) \tag{3}$$

where $\beta = \frac{1}{k_B T}$ and k_B being the Boltzmann constant. For the remainder of the project we set $J = 1\,\mathrm{J}$ and β will be in units of $\frac{1}{k_B}$ such that $\beta = \frac{1}{T}$ is dimensionless.

KT phase transition Unlike the Ising model, the XY model does not have a 2nd order phase transition.

2 Numerical Methods

2.1 Monte Carlo Metropolis-Hastings Algorithm

1. Calculate E and M for the initial lattice configuration.
2. Perform a lattice sweep by iterating over all lattice sites. For every site i do:
   a) Propose a new angle $\theta_i \in [0, 2\pi)$ from a uniform distribution.
   b) Calculate $\Delta H = \Delta E$ and ΔM for the proposed new state.
   c) Accept or reject state with propability $P = \min(1, \exp(-\beta \Delta H))$
3. Update the observables $E \mathrel{+}= \Delta E$ and $M \mathrel{+}= \Delta M$ and add them to the result set.
4. Repeat from 2. for a total of N sweeps.

2.2 Bootstrap Analysis

Since the Metropolis-Hastings algorithm scales with the number of lattices sites, it is computationally impractical to run the Metropolis-Hastings algorithm for very long times. To resolve this, one might use bootstrap sampling to obtain more measurements than were simulated.

2.3 Implementation

3 Results

The following results were obtained for a run on the *JUSUF*[1] cluster with 2 nodes and 4 tasks per node. The simulation ran for $N = 1\,200\,000$ sweeps on lattice sizes $L \in \{32, 48, \ldots, 272\}$ and the bootstrap parameters were $A = N$ and $B = 200\,000$.

3.1 Energy per Spin

As the total energy of the system as defined in eq. (1) scales with the number of lattice sites, it is often more insightful to observe the energy per spin

$$E = -\frac{1}{L^2} \sum_{\langle i,j \rangle} \cos\left(\Delta\theta\right) \tag{4}$$

which has been plotted in fig. 1.

For low temperatures we have a quasi-ordered state where the spins mostly align. Just like in the Ising model the energy per spin is -2.0 when extrapolating to $T = 0$. With increasing temperature the energy slowly vanishes until it asymptotically aproaches 0 for big T.

3.2 Magnetization per Spin

The absolute total magnetization per spin for the system is given by

$$|M|^2 = \frac{1}{L^2} \left(\left(\sum \cos\theta_i \right)^2 + \left(\sum \sin\theta_i \right)^2 \right) \tag{5}$$

and has been plotted in fig. 2.

For low temperature the magnetzation tends to 1 which confirms the existance of a quasi-ordered low temperature state. With increasing temperature the magnetization decreases steadily at first and then rapdily until slowly levels out in the unordered high

[1] `https://www.fz-juelich.de/en/ias/jsc/systems/supercomputers/jusuf`

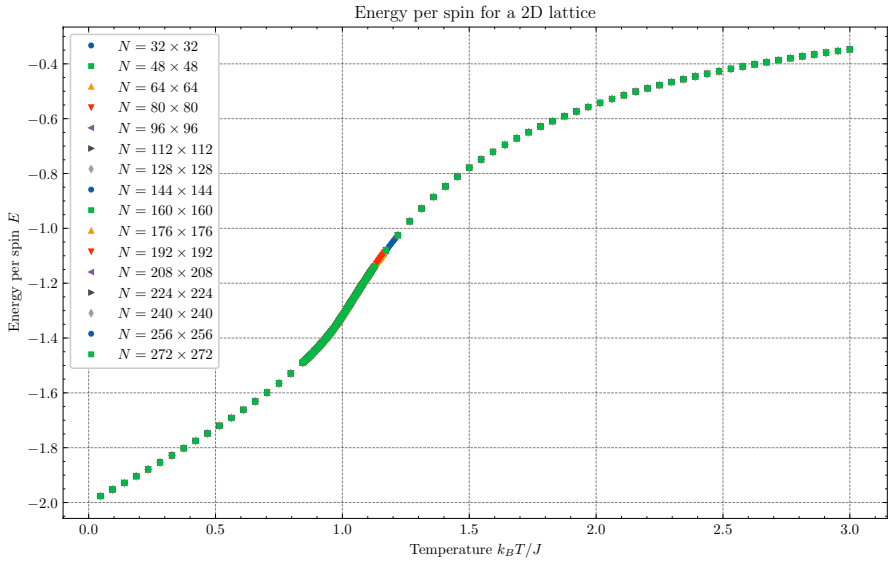

Figure 1: Plot of the temperature dependence of the energy per spin E (eq. (4)) for lattice sizes $L \in \{32, 48, \ldots, 272\}$. For small T the energy tends to -2 while for big temperatures the energy asymptotically approaches 0.

temperature state. One can also see some finite size effects. For increasing lattice sizes the form of the curve becomes more pronounced.

3.3 Specific Heat per Spin

The specific heat of the system can be found by evaluating

$$C_V = \frac{\langle E^2 \rangle - \langle E \rangle^2}{T^2} \tag{6}$$

and has bee plotted logarithmically in fig. 3.

The specific heat is small for low temperatures and even smaller for big temperatures. Near the critical temperature there is a small peak which shrinks for increasing lattice sizes. The position of this peak moves towards smaller temperatures when the lattice size is increased.

3.4 Magnetic Susceptibility per Spin

The mangetic susceptibility of the system can be found by evaluating

$$\chi = \frac{\langle M^2 \rangle - \langle M \rangle^2}{T} \tag{7}$$

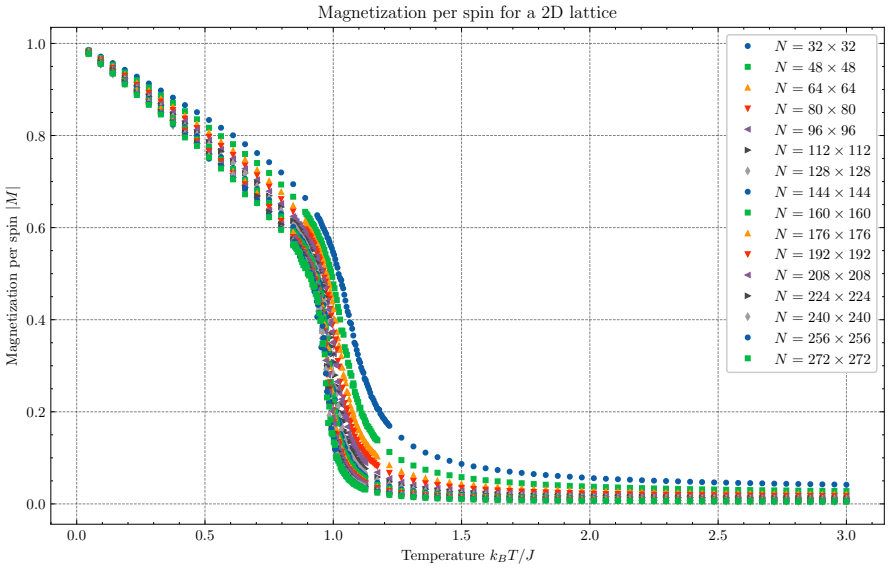

Figure 2: Plot of the temperature dependence of the magnetization per spin $|M|^2$ (eq. (5)) for lattice sizes $L \in \{32, 48, \ldots, 272\}$. For small T the magnetization tends to 1 which indicates an ordered state. For big temperatures the magnetzation goes to 0 which indicates a unordered state.

and has bee plotted logarithmically in fig. 4.

The magnetic susceptibility is small for low and high temperatures. There exists a peak near the critical temperature which slowly moves left for increasing lattice sizes while the magnitude of the peak slowly shrinks.

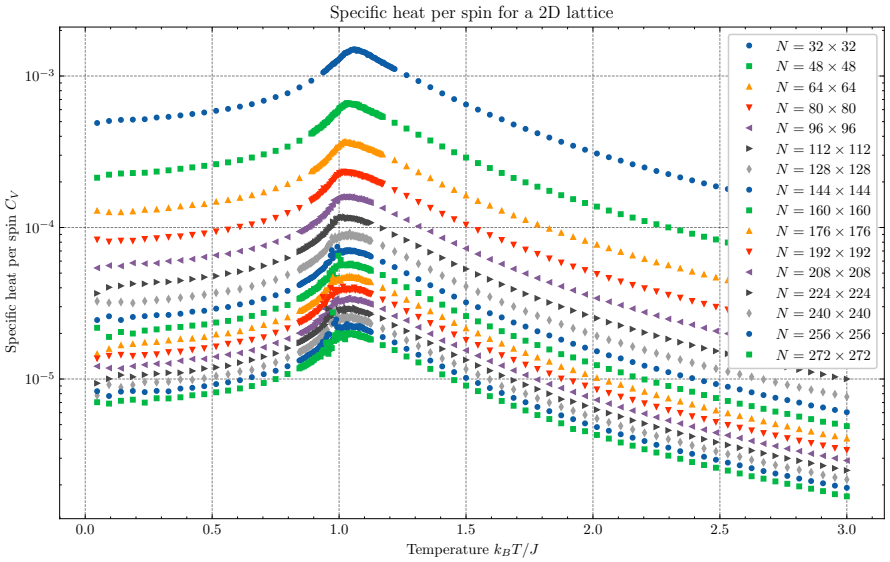

Figure 3: Plot of the temperature dependence of the specific heat per spin C_V (eq. (6)) for lattice sizes $L \in \{32, 48, \ldots, 272\}$. The specific heat generally shrinks with increasing lattice size and tends to 0 for very small and big temperatures. There is peak near the critical temperature T_C which shifts to the left for increasing lattice sizes.

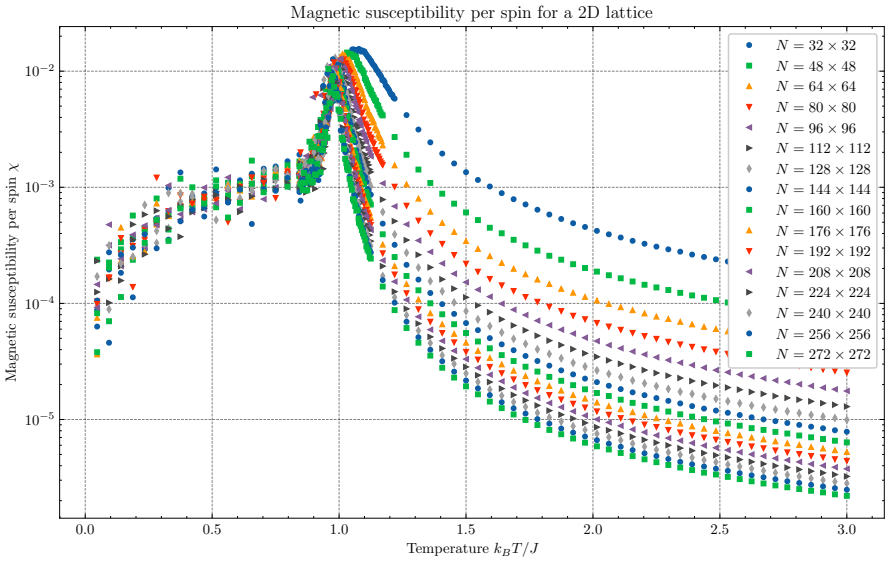

Figure 4

3.5 Critical Temperature T_C

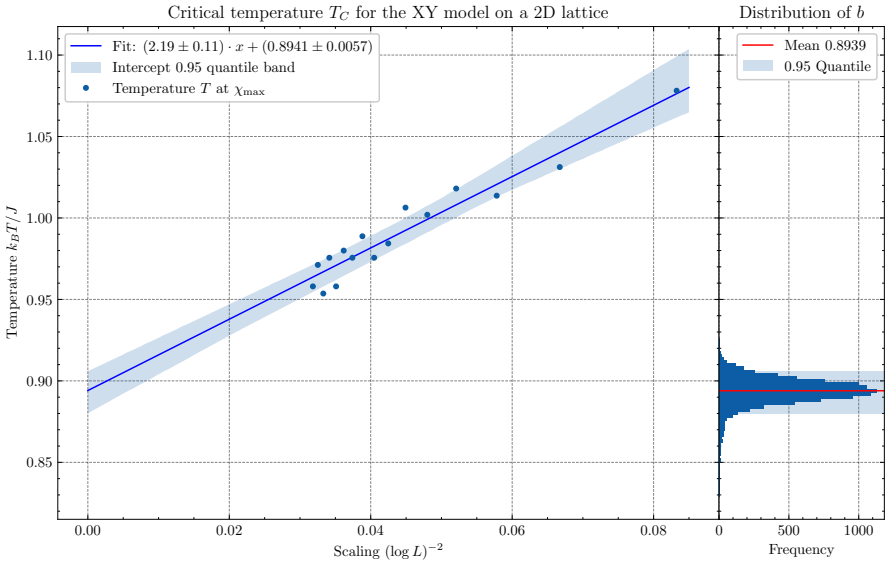

Figure 5

To find the critical temperature where the the KT phase transition takes place one can use the magnetic susceptibility from section 3.4. As shown by Chung (1999) there exists a shifted temperature T^* which asymptotically approaches the critical temperature T_C for increasing lattice sizes

$$T^*(L) \approx T_C + \frac{\pi^2}{4c(\ln L)^2} \tag{8}$$

(Chung, 1999, eq. 3). To confirm the correlation of lattice size and shifted temperature we now take the maximum magnetic susceptibility $\chi_{\max}$ per lattice size from fig. 4 and plot the temperature T where it occurs against $(\ln L)^{-2}$ (fig. 5).

We fitted an ordinary linear regression model using the least square method against our measurements. This fits our data well and confirms the correlation of lattice size and shifted temperature. To estimate our uncertainties we used a parametric bootstrap approach by resampling 10 000 times from our measurements and redoing our linear regression model each time. As seen on the right side in fig. 4 the distribution of intercepts b follows a gaussian distribution and therefore the CLT. Taking the standard deviation as the 95 % confidence band we get our estimate for the critical temperature

$$T_C = 0.8941(57). \tag{9}$$

We can now compare our results with some literature values

- In Hsieh et al. (2013) the authors used a GPU based Monte Carlo approach to estimate the critical temperature to $T_C = 0.8935(1)$.

- In Olsson (1995) the authors used a CPU based Monte Carlo approach to estimate the critical temperature to $T_C = 0.892\,13(10)$.
- A theoretical transfer matrix approach employed by Mattis (1984) lead to a critical temperature of $T_C \approx 0.8916$.

As these estimates lie within the confidence interval of our simulation we may conclude that our simulation was a success. It is of note that our uncertainty is much larger than those of others as we were more constrained by our computational resources and time available.

3.6 Vortices

3.7 Performance

3.7.1 Schedueling

3.7.2 Test

3.7.3 Critical slowing down

4 Conclusion

In this work we were able to simulate the 2D XY model using a numerical Monte Carlo approach. For this we used the Metropolis-Hastings algorithm (section 2.1), bootstrapping (section 2.2) and distributed computing techniques. The simulation ran on the *JSUSUF* cluster at *FZ Jülich* and helped us study the observables E, $|M|^2$, C_V and χ.

In section 3.5 we used the shifted temperature in eq. (8) to get an estimate for the critical temperature

$$T_C = 0.8941(57). \tag{10}$$

The uncertainty is the 95 % confidence band obtained from bootrapping the intercept of our linear regression model using a least square algorithm. As discussed in section 3.5 our estimate is compatible with existing literature.

List of Figures

1 Temperature dependence of the energy per spin E 3
2 Temperature dependence of the magnetzation per spin $|M|^2$ 4
3 Temperature dependence of the specifc heat per spin C_V 5
4 Temperature dependence of the mangetic susceptibility per spin χ 5
5 Obtaining the critical temperature T_C by plotting the temperature T at $\chi_{\max}$ against $(\ln L)^{-2}$ 6

References

S. G. Chung. Essential finite-size effect in the two-dimensional xy model. *Phys. Rev. B*, 60:11761–11764, Oct 1999. doi: 10.1103/PhysRevB.60.11761. URL https://link.aps.org/doi/10.1103/PhysRevB.60.11761.

Yun-Da Hsieh, Ying-Jer Kao, and Anders W Sandvik. Finite-size scaling method for the berezinskii–kosterlitz–thouless transition. *Journal of Statistical Mechanics: Theory and Experiment*, 2013(09):P09001, September 2013. ISSN 1742-5468. doi: 10.1088/1742-5468/2013/09/p09001. URL http://dx.doi.org/10.1088/1742-5468/2013/09/P09001.

Daniel C. Mattis. Transfer matrix in plane-rotator model. *Physics Letters A*, 104(6):357–360, 1984. ISSN 0375-9601. doi: https://doi.org/10.1016/0375-9601(84)90816-8. URL https://www.sciencedirect.com/science/article/pii/0375960184908168.

Peter Olsson. Monte carlo analysis of the two-dimensional xy model. ii. comparison with the kosterlitz renormalization-group equations. *Phys. Rev. B*, 52:4526–4535, Aug 1995. doi: 10.1103/PhysRevB.52.4526. URL https://link.aps.org/doi/10.1103/PhysRevB.52.4526.